Materials Chemistry and Physics 207 (2018) 359–366

Contents lists available at ScienceDirect

Materials Chemistry and Physics

journal homepage: www.elsevier.com/locate/matchemphys

Monodisperse-porous titania microspheres and their gold decorated forms as new photocatalysts for dye degradation in batch fashion

Kadriye Özlem Hamaloğlu [a], Ebru Sağ [b], Aykut Bilir [c], Ali Tuncel [a, c, *]

[a] Hacettepe University, Chemical Engineering Department, Ankara, Turkey
[b] Cumhuriyet University, Chemical Engineering Department, Sivas, Turkey
[c] Hacettepe University, Division of Nanotechnology and Nanomedicine, Ankara, Turkey

HIGHLIGHTS

- Monodisperse porous titania microspheres were synthesized as a new photocatalyst.
- AuNP decorated forms were obtained with AuNPs by Turkevich and Martin methods.
- Photocatalytic degradation of textile dye in batch mode.
- A new type of decolorization including two stages, initial adsorption and degradation.
- Complete decolorization time was reduced 50% by Martin AuNP decorated form.

GRAPHICAL ABSTRACT

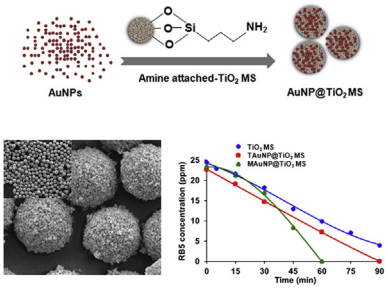

ARTICLE INFO

Article history:
Received 31 December 2016
Received in revised form
22 December 2017
Accepted 25 December 2017
Available online 30 December 2017

Keywords:
Titania microspheres
Gold decorated titania microspheres
Photocatalysis
Dye degradation
Remazol Black 5

ABSTRACT

A new photocatalyst in the form of "*monodisperse-porous titania microspheres*" 5 μm in size, was synthesized by a developed staged-shape template hydrolysis and condensation protocol. Different from the batch-decolorization studies performed with the "*non-porous titania nanoparticles*", a two-stage decolorization process including a fast initial dye adsorption and a relatively slower photodegradation was observed with the proposed photocatalyst. Higher initial decolorization rate was achieved due to the fast dye adsorption onto the porous titania microspheres with higher surface area with respect to "*non-porous titania nanoparticles*" commonly employed as photocatalyst in similar decolorization studies. Moreover, gold decorated forms of monodisperse-porous titania microspheres were also synthesized. Higher decolorization rates with respect to the bare titania microspheres were achieved with the gold decorated forms at neutral pH. Gold decorated photocatalyst synthesized using gold nanoparticles with lower size provided 50% higher decolorization rate due to their better electron transfer characteristics.

1. Introduction

In the last century, conventional physical, biological and chemical processes were used to remove organic compounds from contaminated water [1,2]. Due to the limitations of these processes, a lot of research has been done in the last decades about a new class of oxidation processes which is called as Advanced Oxidation

* Corresponding author. Hacettepe University, Chemical Engineering Department, Ankara, Turkey.
E-mail address: atuncel@hacettepe.edu.tr (A. Tuncel).

https://doi.org/10.1016/j.matchemphys.2017.12.065
0254-0584/

Processes (AOPs) [3,4]. AOPs consists of different processes like; chemical oxidation processes (ozone (O_3), ozone/hydrogen peroxide(O_3/H_2O_2), Fenton photochemical oxidation processes (UV/O_3, UV/H_2O_2) and photocatalytic processes (UV/TiO_2) [1,4]. Each process is based on the formation of hydroxyl radicals and reaction of these hydroxyl radicals with organic contaminants. Heterogeneous photocatalysis, in which semiconductor metal oxides are used instead of oxidants like H_2O_2 and O_3 with UV light, is a promising method for the degradation of organic compounds [1]. Among the semiconductors that have been used for photocatalysis, titania (TiO_2) is the most suitable one due to high activity, low cost and non-toxicity [5]. Specific surface area and crystallinity are the most important factors affecting on the photocatalytic activity [6]. Accordingly, titania nanoparticles have attracted great interest because of its usability in heterogeneous photocatalysis.

The reason of using catalysts in small size is to obtain higher surface areas as the catalytic reactions occur on the surface of the particles. Unfortunately, the particles in nanometer scale are not stable, they tend to agglomerate and it is a serious problem to remove the nanoparticles from solutions after the catalytic reaction [7]. To overcome these disadvantages: 1) different supports with high surface areas can be used to keep the active catalyst in the dispersed state in the reaction medium [7], 2) porous TiO_2 microspheres (TiO_2 MS) with high surface area, easy removal, controllable shape and size can be used. In order to synthesize monodisperse porous titania beads, polymeric templates, which controls the morphological properties such as pore size, outer shape and size, are used [8].

Staged-shape template hydrolysis and condensation protocol is a synthesis method allowing the synthesis of micron-size, porous TiO_2 MS with a prescribed size [9]. The size of monodisperse TiO_2 MS can be controlled by the selection of the polymer based template particles used as starting material in the synthesis. Moreover, the porous characteristics (i.e. the porosity, the pore-size distribution and the specific surface area) of TiO_2 MS can be also adjusted by tuning the porous properties of seed polymer particles [9]. Hence, the monodisperse-porous TiO_2 MS with prescribed size and porous properties can be synthesized by using staged-shape template hydrolysis and condensation protocol. In this study, this synthesis method was preferred for obtaining monodisperse, micron size and porous titania spheres as an easily removable photocatalytic material more resistant to aggregation in the reaction medium and with higher surface area with respect to conventional titania nanoparticles.

Remazol Black 5 (RB5) is an azo dye which is non-biodegradable under aerobic conditions and is very stable due to its complex molecular structure [10,11]. Under unaerobic conditions azo dyes can be degraded but hazardous and carcinogenic aromatic amines are formed as degradation products [11]. By using titania photocatalysts in nanometer range, complete degradation of RB5 in the aqueous medium was achieved by different groups [12,13]. The results showed that operational parameters like pH, catalyst concentration, crystal composition, specific surface area, initial reactant concentration, calcination temperature and light intensity play an important role on the photocatalytic activity [14]. In order to improve their photochemical properties, many researchers have focused on the enhancement of photocatalysis by doping noble metals on TiO_2 like gold (Au) [15,16].

Various photocatalysts were prepared based on Au-TiO_2 composites. Functionalized silicate sol-gel-supported TiO_2-Au core-shell nanomaterials and their photoelectrocatalytic activity was investigated [17]. TiO_2–Au nanocomposite materials were embedded in polymer matrices and used in the photocatalytic reduction of nitrite to ammonia [18]. Titanium dioxide–gold nanocomposite materials were embedded in silicate sol–gel film and used as catalyst for simultaneous photodegradation of chromium and methylene blue [19].

In our first study, monodisperse-porous TiO_2 MS were synthesized by a recently developed sol-gel templating method using -SO_3Na attached-polymethacrylate microspheres as a template [9]. In the referred study, the usability of bare TiO_2 MS for photocatalytic dye degradation was briefly shown. In our second study, gold decorated forms of monodisperse-porous TiO_2 MS were obtained and evaluated as a photocatalyst in "*Microfluidic, Photocatalytic Packed Bed Reactor (MPPBR)*" for continuous photocatalytic dye degradation [20]. In the present study, the photocatalytic activity of monodisperse-porous TiO_2 MS decorated with gold nanoparticles (AuNPs) with different sizes (i.e. obtained by Martin and Turkevich methods) were investigated in a "*batch photocatalytic reactor*" by the degradation of a textile dye, RB5 under UV-irradiation, using bare-TiO_2 MS as a reference photocatalyst. The effects of operating conditions like pH, initial dye concentration, photocatalyst concentration, crystal structure and surface area of photocatalyst on the conversion and photodegradation rate of RB5 were investigated. The effects of AuNP size and AuNP loading on the photocatalytic activity of monodisperse-porous TiO_2 MS were also defined in the batch photocatalytic reactor.

2. Experimental

2.1. Materials

All the chemicals used for the preparation of sodium sulfonate attached-poly(3-chloro-2-hydroxypropyl methacrylate-co-ethylene glycol dimethacrylate) (-SO_3Na attached-poly(HPMA-Cl-co-EDMA)) microspheres and TiO_2 MS were purchased from Sigma Chemical Co., St. Louis, MO, USA, as reported in our earlier study [9]. For the derivatization of monodisperse-porous TiO_2 MS with amine groups aminopropyltriethoxysilane (APTES) and triethylamine (TEA) were purchased from Sigma Chemical Co., St. Louis, MO, USA. All the chemicals used for the synthesis of AuNPs, were purchased from Sigma Chemical Co., St. Louis, MO, USA, as given in our previous study [20]. Ethanol (EtOH, HPLC grade, Merck A.G., Darmstadt, Germany), tetrahydrofuran (THF, HPLC grade, Aldrich) and isopropanol (Iso-PrOH, HPLC grade, Aldrich) were used as solvents. The dye used in the photocatalytic activity runs, RB5 was purchased from Aldrich. Distilled deionized (DDI) water (Direct-Q 3 UV (Type 1), Millipore, USA) with a resistivity of 18 MΩ cm was used in all synthetic studies.

2.2. Preparation of bare titania and AuNP decorated TiO_2 MS

TiO_2 MS were synthesized by sol-gel templating method using -SO_3Na attached-poly(HPMA-Cl-co-EDMA) microspheres as template, as reported earlier [20]. Before the AuNP decoration, primary amine groups were attached onto the TiO_2 MS by the reaction between ethoxysilane groups of APTES and hydroxyl groups of TiO_2 MS [20]. AuNPs were synthesized by using different reducing agents as trisodium citrate and sodium borohydride according to the methods given in our previous study [20]. For AuNP decoration, amine attached TiO_2 MS were put into AuNP solutions obtained by Turkevich or Martin method and stirred at 250 rpm for 6 h at room temperature [20]. To change the Au loading (2.5, 5.0, 10.0% w/w) on the TiO_2 MS, different amounts of amine attached TiO_2 MS were put into the same volume of AuNP solutions (0.2, 0.1, 0.05 g to 24 mL Turkevich AuNP solution; 0.16, 0.08, 0.04 g to 80 mL Martin AuNP solution).

2.3. Photocatalytic degradation of RB5 dye in batch fashion

The photocatalytic activity of bare and AuNP decorated TiO_2 MS were determined using a textile dye, RB5 within a system as described in our previous study [9]. Briefly, the photocatalyst was dispersed in an aqueous dye solution (100 mL) at a certain pH, by ultrasonication for 5 min at 200 W. The reaction mixture in a beaker (250 mL) was irradiated from the top with a UV light-source (Osram, Ultra-vitalux lamp, 300 W). The photocatalytic runs were performed using magnetic stirring (300 rpm) at 25 °C in a closed box including a temperature-control system. The concentration of RB5 dye was determined by absorbance measurement at 598 nm using UV-Vis spectrophotometer (UV-1601, Shimadzu, Japan). The effect of calcination temperature (450, 500, 550, 600 °C), pH of reaction medium (3.5, 5.0, 7.0, 9.0), catalyst concentration (20, 40, 80 mg), RB5 dye concentration (12.5, 25.0, 50.0 ppm) and Au loading (2.5, 5.0, 10.0% w/w) on the photocatalytic activity were investigated.

2.4. Characterization

The size distribution properties and the surface morphology of poly(HPMA-Cl-co-EDMA) microspheres, bare and AuNP decorated TiO_2 MS were investigated by scanning electron microscopy (SEM; JEM 1200EX, JEOL, Akishima, Tokyo, Japan). The specific surface areas (SSAs) of bare and AuNP decorated TiO_2 MS were determined by surface area and pore size analyzer (Quantachrome, Nova 2200E, UK) using the Brunauer–Emmett–Teller (BET) equation. The functional group content of amine-attached-TiO_2 MS was determined by elemental analysis (Thermo-Scientific, Flash 2000, USA).

3. Results and discussion

3.1. Decoration of monodisperse-porous TiO_2 MS with AuNPs

In this study, monodisperse-porous TiO_2 MS were synthesized by a sol–gel templating method [9]. Prior to gold decoration, the amine functionalized form of bare TiO_2 MS was obtained via a simple reaction between hydroxyl groups of TiO_2 MS and ethoxysilane groups of APTES (Fig. 1). The amine content of functionalized microspheres was determined as 3.2% (% w/w) by elemental analysis. The decoration of bare TiO_2 MS with Turkevich AuNPs or Martin AuNPs was performed by firm contact between the amine functionalized TiO_2 MS and AuNP solution obtained with corresponding methods (Fig. 1). The UV-Vis spectra of Turkevich and Martin AuNP solutions are given in Fig. S1 of Supporting Information. The characteristic surface plasmon bands for the AuNPs 5 nm and 16 nm in size, synthesized with Martin and Turkevich method were observed at 509 and 521 nm, respectively (Fig. S1 of Supporting Information).

The SEM photographs of bare titania, Turkevich AuNP decorated TiO_2 microspheres (TAuNP@TiO_2 MS) and Martin AuNP decorated TiO_2 microspheres (MAuNP@TiO_2 MS) prepared with an Au loading percent of 5% (%w/w) are exemplified in Fig. 2. The difference between the surface morphologies of titania and TAuNP@TiO_2 MS/MAuNP@TiO_2 MS was a visual proof for the presence of AuNPs on the TiO_2 MS. Individual AuNPs could be also distinguished on the SEM photograph of the AuNP decorated TiO_2 MS obtained with the highest magnification.

Au loading percent (% w/w) on TiO_2 MS was varied (2.5, 5.0, 10.0% w/w) by changing the amount of amine attached TiO_2 MS interacted with the same volume of AuNP solution obtained with Turkevich or Martin method. The SSA values of TAuNP@TiO_2 MS and MAuNP@TiO_2 MS are given in Table 1. The SSA values of TAuNP@TiO_2 MS and MAuNP@TiO_2 MS with all Au loading percents were lower than the SSA of bare TiO_2 MS [9]. The decrease in SSA can be explained by the partial filling of mesopores by the AuNPs diffused into the TiO_2 MS. Note that the SSA values obtained for MAuNP@TiO_2 MS were slightly lower with respect to the TAuNP@TiO_2 MS. This result can be explained by more effective diffusion of smaller AuNPs obtained by Martin method into the mesopores of TiO_2 MS. However, SSA values of TAuNP@TiO_2 MS or MAuNP@TiO_2 MS could not be correlated with the Au loading percent. As seen here, the SSA values of MAuNP@TiO_2 MS and TAuNP@TiO_2 MS were only lower with respect to bare TiO_2 MS. An apparent change was not observed in SSA with the increasing AuNP loading for both MAuNP@TiO_2 MS and TAuNP@TiO_2 MS. This result should be probably explained by filling of mesopores and smaller macropores (i.e. the most effective pore fraction controlling the magnitude SSA) even with the lowest AuNP loading (i.e. 2.5% w/w). Hence, further increase in the number of AuNP in the solution should be probably not effective for additional filling of mesopores of TiO_2 MS.

The structure of TAuNP@TiO_2 MS and MAuNP@TiO_2 MS were investigated by XRD and the related patterns are given in Fig. 3. The structure of bare TiO_2 MS was given in our previous study [9]. As seen in Fig. 3, different from the anatase and rutile peaks of bare TiO_2 MS, the characteristic peaks (at 2Θ: 38°, 44°, 64° and 77°) of cubic structure of metallic gold were observed in the XRD patterns of TAuNP@TiO_2 MS and MAuNP@TiO_2 MS. The results showed that AuNPs were successfully incorporated into the TiO_2 MS by both methods without performing a significant change in the crystalline structure of titania. Compared to TAuNP@TiO_2 MS, the intensities of the peaks at 2Θ: 38°, 44°, 64° decreased and the peak at 2Θ: 77° disappeared in the XRD pattern of MAuNP@TiO_2 MS. These results were consistent with the results obtained by Moreau and Bond [21], who also reported that the intensity of characteristic peaks of metallic gold decreased by lowering the size of AuNPs.

3.2. Photocatalytic degradation of RB5 with bare TiO_2 MS in batch reactor

The photocatalytic activity of bare TiO_2 MS was examined by the photocatalytic degradation of an azo dye, RB5. Nitrogen to nitrogen double bonds (-N=N-) in the molecular structure of RB5 are the most active site and can be oxidized either by positive holes or hydroxyl radicals which results in photocatalytic degradation. The decolorization of RB5 dye solution with bare TiO_2 MS was monitored by UV-Vis spectroscopy. Typical UV-Vis spectra obtained at different time intervals during decolorization of RB5 solution are shown in Fig. S2 of Supporting Information. The complete decolorization of RB5 solution was achieved within 120 min under these conditions. The concentration of RB5 dye in the solution at certain times was determined according to the absorbance peak of RB5 at 598 and is given in the inset in Fig. S2.

The effect of calcination temperature on the photocatalytic degradation of RB5 using bare TiO_2 MS as the photocatalyst is given in Fig. 4. In these runs, the starting RB5 dye concentration was 25 ppm. As seen here, a sudden decrease in the dye concentration was observed due to the fast dye adsorption onto TiO_2 MS, at zero reaction time. The initial dye adsorption was characterized by dark-blue colour of photocatalyst microspheres. With the progressing time, RB5 dye concentration decreased mainly due to the photocatalytic degradation taking place on TiO_2 MS. If one compares the results presented in Fig. 4 for TiO_2 MS calcinated at different temperatures, it is evident that calcination at higher temperature has basically a detrimental effect for the RB5 concentration in the decolorization medium. For a certain time, lower RB5 concentration was obtained with TiO_2 MS calcined at lower temperature. However, the RB5 concentration at a certain time is a combined

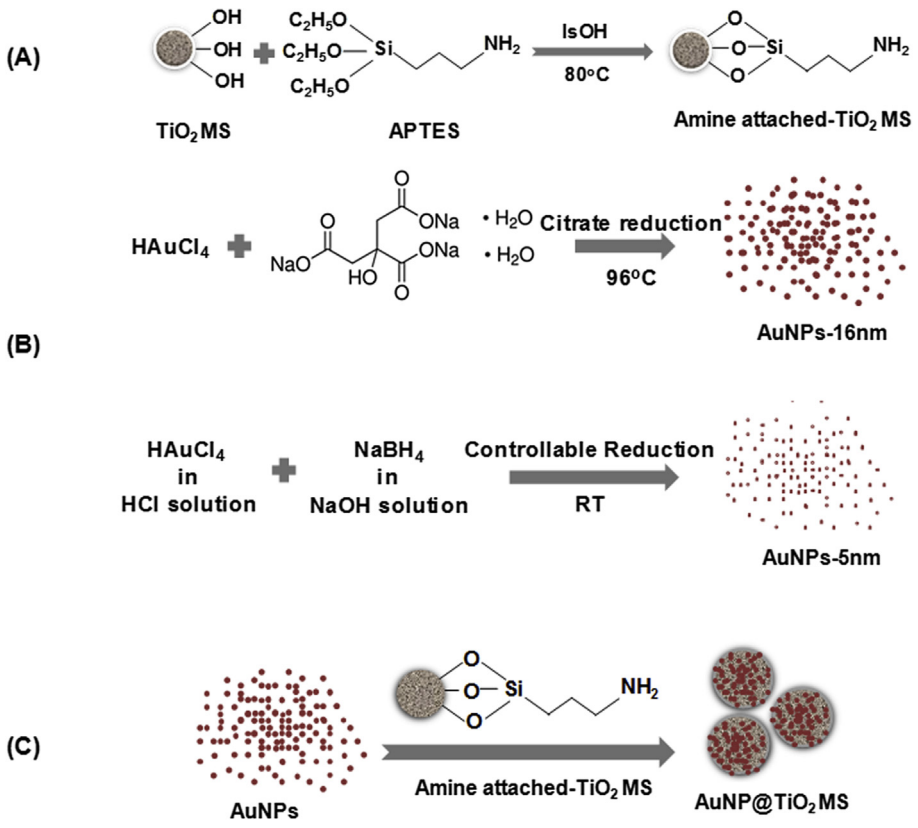

Fig. 1. The synthesis route used for decoration of monodisperse-porous TiO_2 MS by AuNPs. (A) Derivatization of monodisperse-porous TiO_2 MS with APTES (B) Synthesis of AuNPs via Turkevich method and Martin method. (C) Binding of AuNPs onto the monodisperse-porous TiO_2 MS carrying amine functionality.

function of initial dye adsorption and photocatalytic degradation. It was found that SSA of bare TiO_2 MS almost linearly decreased from 91 to 50 m^2/g by increasing the calcination temperature from 450 to 600 °C [9]. In Fig. 4, the highest initial dye adsorption before the irradiation with a UV light-source (i.e. at zero-reaction-time) was obtained with TiO_2 MS calcined at 450 °C and almost 90% (% w/w) of RB5 dye was removed from the solution via adsorption. The lower initial dye adsorption should be explained by the decreasing surface area of TiO_2 MS with the increasing calcination temperature [6]. But, after the zero-reaction-time, lower slope for the dye concentration-time curve (i.e. lower apparent decolorization rate) was observed with TiO_2 MS providing lower RB5 concentration following to the initial dye adsorption. Hence, the lowest slope after the initial dye adsorption was obtained with TiO_2 MS calcined at 450 °C (Fig. 4). The photocatalytic degradation within the porous microspheres should be evaluated as a multi-stage process containing the stages of intraparticular diffusion, adsorption and photocatalytic degradation reaction. The photocatalytic degradation within the porous microspheres is naturally controlled by the stage progressing with the lowest rate. Intraparticular diffusion should be probably the most effective stage for controlling of apparent decolorization rate with the porous photocatalyst particles with a long intraparticular diffusion pathway like 2.7 μm (i.e. the radius of TiO_2 MS). Hence, after the initial, fast dye adsorption period, the slower intraparticular diffusion of RB5 originating from its lower solution concentration is probably the main reason of lower decolorization rate observed with the photocatalyst calcined at lower temperature (Fig. 4).

On the other hand, anatase/rutile ratio was also reported as a critical factor controlling the photocatalytic performance of titania based photocatalyst [22]. The XRD analysis in our previous study showed that the rutile content of TiO_2 MS decreased and the anatase/rutile ratio increased with decreasing calcination temperature [9]. The higher anatase/rutile ratio should be probably another factor providing lower slope for the concentration-time curve after the initial dye adsorption [22].

The variation of RB5 dye concentration with the time during the decolorization of RB5 dye solution with bare TiO_2 MS is given in Fig. 5. As also observed in the previous set, the fast dye adsorption onto the microspheres provided a sudden decrease in the solution concentration of RB5 at zero-reaction time. As anticipated, the initial decrease in the dye concentration was more apparent for lower initial dye concentration. Our results again show that decolorization rate depends on the RB5 concentration obtained at zero-time after the initial dye adsorption stage.

The effect of photocatalyst concentration on the decolorization rate is given in Fig. 6. As seen here, the initial RB5 adsorption onto the TiO_2 MS increased with the increasing amount of TiO_2 MS before the UV-irradiation. The higher surface area obtained with the higher photocatalyst concentration in the reaction medium should be the reason of this behavior. However, the apparent photocatalytic degradation rate at any time was again higher with the lower photocatalyst concentration (Fig. 6). This result should be explained by the faster intraparticular diffusion of RB5 depending upon its higher solution concentration obtained after the initial adsorption of dye onto the photocatalyst before the UV-irradiation.

3.3. Photocatalytic degradation of RB5 dye with AuNP decorated TiO_2 MS in batch reactor

The effect of pH on the decolorization behavior was investigated with TAuNP@TiO_2 MS and MAuNP@TiO_2 MS prepared with 5% (%

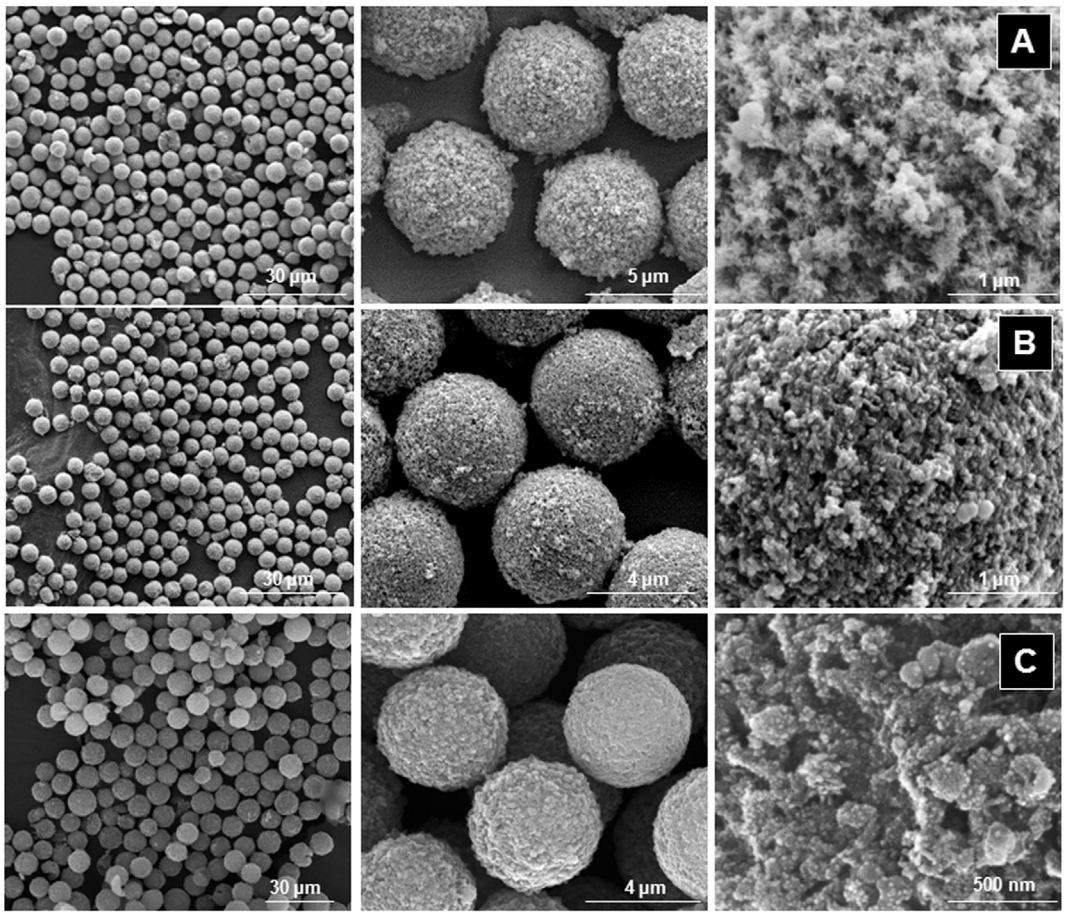

Fig. 2. SEM photographs of (A) bare TiO_2 MS (B) TAuNP@TiO_2 MS (C) MAuNP@TiO_2 MS with an Au loading percent of 5% (%w/w). The scale bar is given on each photograph.

Table 1
Specific surface areas of TAuNP@TiO_2 MS and MAuNP@TiO_2 MS with different Au loading percents.

Turkevich Method		Martin Method	
Au loading percent on TiO_2 microspheres (% w/w)	SSA (m^2/g)	Au loading percent on TiO_2 microspheres (% w/w)	SSA (m^2/g)
0.0	91.0[a]	0.0	91.0[a]
2.5	71.2	2.5	63.2
5.0	72.2[b]	5.0	66.2[b]
10.0	71.6	10.0	65.1

Calcination temperature: 450 °C, a:The values were taken from Ref. [9], b:The values were taken from Ref. [20].

w/w) of Au loading percent, using bare TiO_2 MS as the reference photocatalyst and given in Fig. 7. Au loading percent was defined as the weight ratio of AuNPs to the amine functionalized TiO_2 MS in the binding medium. The curves obtained with the bare titania are shown by solid lines, while the dotted lines were used for the curves with TAuNP@TiO_2 MS and MAuNP@TiO_2 MS. For the synthesis of AuNP decorated photocatalysts, AuNPs 16 and 5 nm in size were synthesized by applying the Turkevich and Martin methods, respectively. Then, TAuNP@TiO_2 MS and MAuNP@TiO_2 MS were obtained by the immobilization of AuNPs 16 and 5 nm in size on the bare TiO_2 MS, respectively. All photocatalytic runs were performed using the TiO_2 MS calcined at 450 °C. As seen in Fig. 7, the decolorization performance of TAuNP@TiO_2 MS was compared with the bare TiO_2 MS at acidic, neutral and alkaline pH (i.e. pH 3.5, 7.0 and 9.0). However, an enhancement in the decolorization rate with respect to the bare titania was only observed at neutral pH using TAuNP@TiO_2 MS. For this reason, MAuNP@TiO_2 MS were tried at neutral pH.

The point of zero-charge for bare titania is obtained at pH 6.5. Under acidic conditions ($pH \leq 6.5$), the TiO_2 MS are protonated, while under alkaline conditions ($pH \geq 6.5$) they are deprotonated. A strong interaction occurred between the SO_3^- groups of RB5 and positively charged bare TiO_2 MS in an acidic medium which results in higher adsorption of RB5 onto bare TiO_2 MS (i.e. the solid blue line in Fig. 7). The initial dye adsorption was also reasonably higher with respect to that observed with the conventional non-porous titania nanoparticles (P25 Degussa, U.S.A.), particularly in the acidic decolorization medium [9]. When compared to the bare TiO_2 MS, less amount of RB5 was adsorbed by TAuNP@TiO_2 MS particularly in the acidic region (i.e. pH 3.5) at zero-reaction time (i.e. the dotted lines Fig. 7). The reasons of lower adsorption are: 1) less positively charged microspheres

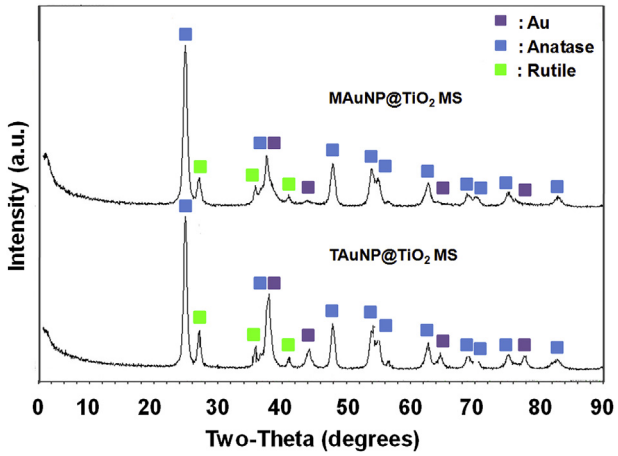

Fig. 3. XRD patterns of TAuNP@TiO_2 MS and MAuNP@TiO_2 MS with an Au loading percent of 5% (%w/w).

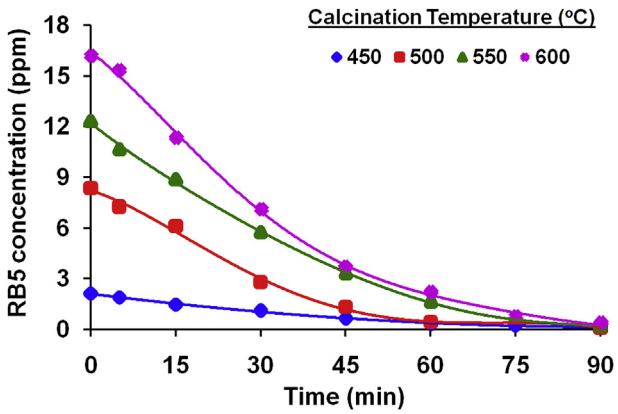

Fig. 4. Effect of calcination temperature on the photocatalytic degradation of RB5 dye with bare TiO_2 MS. (Conditions: catalyst amount: 80 mg, RB5 dye solution: 25 ppm, 100 mL, pH: 3.5).

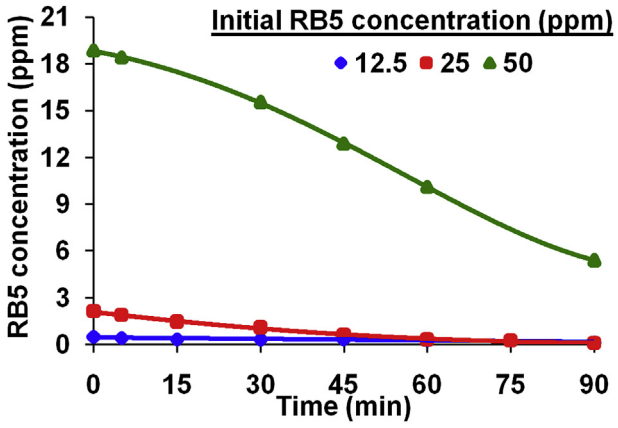

Fig. 5. Effect of initial RB5 concentration on the photocatalytic degradation rate of RB5 dye with bare TiO_2 MS. (Conditions: catalyst amount: 80 mg, calcination temperature: 450 °C, pH: 3.5).

due to the negatively charged citrate ions on AuNPs and 2) lower SSA because of loading Turkevich AuNPs particularly into the mesopores of bare TiO_2 MS. The complete decolorization occurred within 90 min with both photocatalyst at pH 3.5 and no

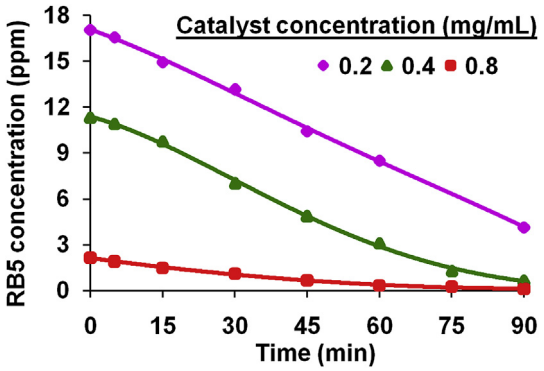

Fig. 6. Effect of catalyst concentration on the photocatalytic degradation rate of RB5 with bare TiO_2 MS. (Conditions: calcination temperature: 450 °C, RB5 dye solution: 25 ppm, 100 mL, pH: 3.5).

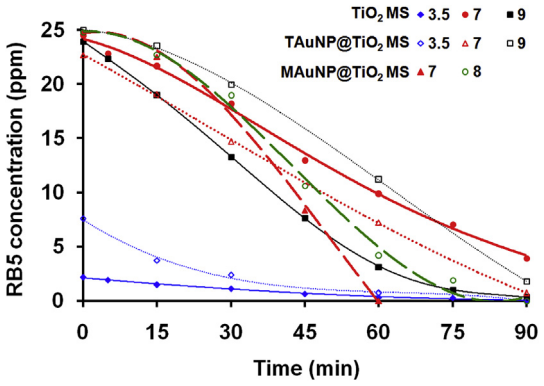

Fig. 7. Effect of pH on the photocatalytic degradation rate of RB5 dye with bare TiO_2 MS, TAuNP@TiO_2 MS and MAuNP@TiO_2 MS. (Conditions: solid lines: bare TiO_2 MS, dotted lines with short segment: TAuNP@TiO_2 MS, dotted lines with long segment: MAuNP@TiO_2 MS catalyst amount: 80 mg, Au loading percent (% w/w): 5%, RB5 dye solution: 25 ppm, 100 mL).

enhancement with the TAuNP@TiO_2 MS was observed. The initial dye adsorption at pH 9 was very low since both TiO_2 MS and dye were negatively charged. Moreover, the reason for lower decolorization rate at pH 9 with the TAuNP@TiO_2 MS compared to the bare titania can be attributed to the high negative charge on the microspheres in the alkaline medium due to the citrate ions on the immobilized AuNPs.

Owing to the presence of the lowest charge on TiO_2 MS at pH 7, the lowest initial dye adsorption was obtained at this pH and then a high RB5 solution concentration immediately after contacting the reaction mixture with the bare TiO_2 MS was measured. The complete decolorization was achieved with the TAuNP@TiO_2 MS within 90 min while it was not obtained at pH 7 with the bare TiO_2 MS. Then, an apparent enhancement in the photocatalytic activity was only observed at pH 7, with the TiO_2 MS decorated with citrate stabilized Turkevich AuNPs. AuNPs on TiO_2 MS should increase the photocatalytic activity by decreasing the band-gap of TiO_2 MS [23]. As the band-gap of the TiO_2 MS decreases, the light absorption increases which results in an enhancement in the photocatalytic activity.

As also seen in Fig. 7, the highest decolorization rate in this study was achieved with the MAuNP@TiO_2 MS in which the AuNP size was smaller (red dotted line with larger segments) at pH 7. Kamat et al. reported that small AuNPs induce larger shifts in the Fermi level than the large particles do, which means that the size of

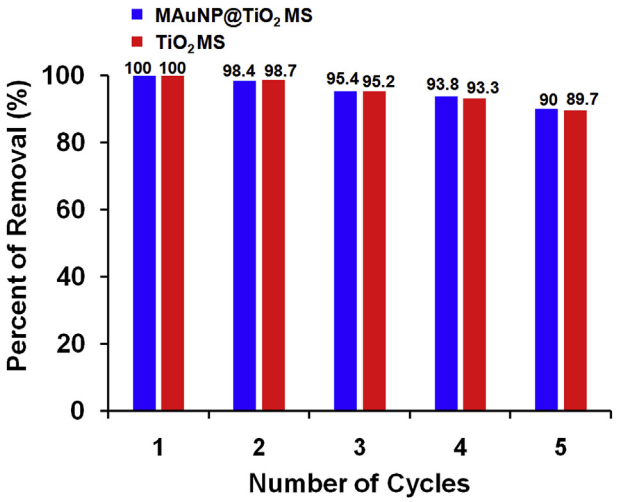

Fig. 8. Reusability of bare TiO_2 MS and MAuNP@TiO_2 MS in the decolorization of RB5 dye solution. (Conditions: catalyst amount: 80 mg, Au loading percent (%w/w): 5%, RB5 dye solution: 25 ppm, 100 mL, pH: 7).

AuNPs directly affects on the photocatalytic activity [23].

The variation of RB5 concentration with time during the decolorization with MAuNP@TiO_2 MS prepared by changing the Au loading percent is given in Fig. S3 of Supporting Information. As seen here, an apparent enhancement in the photocatalytic activity was obtained with the AuNP loading percent of 5% (% w/w) for MAuNP@TiO_2 MS. The excess blocking of photocatalytic active sites and the decrease in the light permeability due to the high surface concentration of AuNPs should be evaluated as possible reasons involving lower decolorization rate with 6 and 10% (% w/w) of AuNP loading.

The reusability of bare TiO_2 MS and MAuNP@TiO_2 MS with the highest photocatalytic activity (Au loading percent: 5% (%w/w)) were investigated at pH 7 by performing five successive batch-decolorization runs under identical conditions. The decolorization times with bare TiO_2 MS and MAuNP@TiO_2 MS were 90 and 60 min, respectively. After each experiment, the photocatalysts were recovered by rinsing with water for several times for reuse. The percent of removal values for RB5 dye achieved after each cycle are given in Fig. 8. At the end of the fifth cycle, only around 10% of decrease in the percent of dye-removal with both photocatalysts was observed. This decrease was ascribed to the adsorption of degradation products on the photoactive sites of bare TiO_2 MS and MAuNP@TiO_2 MS.

The Schematic representation for the photocatalytic degradation of RB5 and photoinduced charge-transfer mechanism for MAuNP@TiO_2 MS is given in Fig. 9. As seen here, an electron of anatase TiO_2 MS was promoted from the valence band to the conduction band forming behind a hole in the valence band by the UV excitation [24]. The hole accumulated at the valence band of TiO_2 MS leads to the production of surface hydroxyl radicals which cause oxidative decomposition of RB5 [25]. When coupling AuNP with TiO_2 MS, photogenerated electrons flow toward AuNP and accumulated there [24,26,27]. Then, the superoxide and hydroxyl radical production rates were enhanced [25]. Hence, the photocatalytic oxidation process was accelerated by these active species.

4. Conclusion

In this study, AuNP decorated monodisperse-porous TiO_2 MS were synthesized by the decoration of AuNPs on amine-attached TiO_2 MS obtained by a recently introduced "multistage sol-gel templating protocol". The photocatalytic activity of monodisperse-porous bare TiO_2 MS could be markedly increased by the decoration with low sized AuNPs in the batch decolorization taking place at neutral pH. In other words, the time necessary for complete decolorization in batch fashion was approximately reduced from 90 to 60 min.

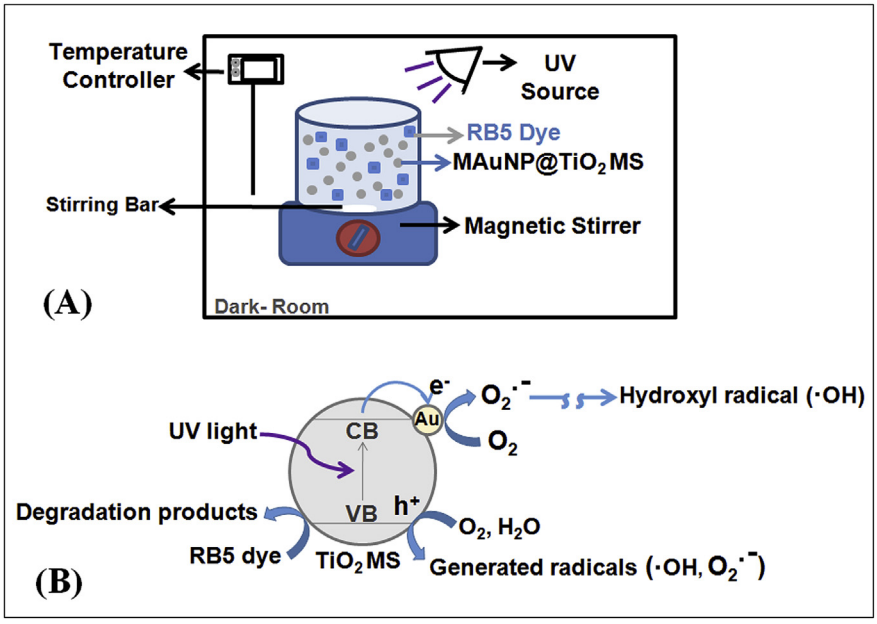

Fig. 9. Schematic representation for the photocatalytic degradation of RB5 and photoinduced charge-transfer mechanism for MAuNP@TiO_2 MS. (A) Representation for the photocatalytic degradation of RB5 (B) Representation for the photoinduced charge-transfer mechanism for MAuNP@TiO_2 MS.

Funding

This research did not receive any specific grant from funding agencies in the public, commercial, or not-for-profit sectors.

Conflict of interest statement

Prof. Ali Tuncel is a full member of Turkish Academy of Sciences (TUBA). The other authors whose names are listed immediately below declare that they have no conflict of interest.

Author names: Kadriye Özlem Hamaloğlu, Ebru Sağ, Aykut Bilir, Ali Tuncel.

Acknowledgements

Special thanks are extended to Turkish Academy of Sciences (TUBA) for the research support provided to Prof. Ali Tuncel as a full member.

Appendix A. Supplementary data

Supplementary data related to this article can be found at https://doi.org/10.1016/j.matchemphys.2017.12.065.

References

[1] H.F. Kambala, V.S.R. Srinivasan, M.D. Rajarathnam, R. Naidu, Tailored titanium dioxide photocatalysts for the degradation of organic dyes in wastewater treatment: a review, Appl. Catal. Gen. 359 (2009) 25–40.
[2] J.L. Gong, B. Wang, G.M. Zeng, Removal of cationic dye from aqueous solution using magnetic multi-wall carbon nanotube nanocomposite as adsorbent, J. Hazard Mater. 164 (2009) 1517–1522.
[3] S. Rashidi, M. Nikazar, A.V. Yazdi, R. Fazaeli, Optimized photocatalytic degradation of reactive blue 2 by TiO_2/UV process, J Environ Sci Heal A 49 (2014) 452–462.
[4] M. Muruganandham, R.P.S. Suri, M. Sillanpää, J.J. Wu, B. Ahmmad, S. Balachandran, M. Swaminathan, Recent developments in heterogeneous catalyzed environmental remediation processes, J. Nanosci. Nanotechnol. 14 (2014) 1898–1910.
[5] A. Fujishima, X. Zhang, Titanium dioxide photocatalysis: present situation and future approaches, Cr Acad Sci II C 9 (2006) 750–760.
[6] J. Lee, M. Orilall, S. Warren, M. Kamperman, F. DiSalvo, U. Wiesner, Direct access to thermally stable and highly crystalline mesoporous transition-metal oxides with uniform pores, Nat. Mater. 7 (2008) 222–228.
[7] M.H. Baek, J.W. Yoon, J.S. Hong, J.K. Suh, Application of TiO_2-containing mesoporous spherical activated carbon in a fluidized bed photoreactor-Adsorption and photocatalytic activity, Appl. Catal. Gen. 450 (2013) 222–229.
[8] R.A. Caruso, Nanocasting and nanocoating, Top. Curr. Chem. 226 (2003) 91–118.
[9] K.Ö. Hamaloğlu, B. Çelebi, E. Sağ, A. Tuncel, A new method for the synthesis of monodisperse-porous titania microbeads by using polymethacrylate microbeads as template, Micropor Mesopor Mat 207 (2015) 17–26.
[10] M.H. Habibi, A. Hassanzadeh, S. Mahdavi, The effect of operational parameters on the photocatalytic degradation of three textile azo dyes in aqueous TiO_2 suspensions, J Photoch Photobio A 172 (2005) 89–96.
[11] E. Bizani, K. Fytianos, I. Poulios, V. Tsiridis, Photocatalytic decolorization and degradation of dye solutions and wastewaters in the presence of titanium dioxide, J. Hazard Mater. 136 (2006) 85–94.
[12] P. Qu, J. Zhao, T. Shen, H. Hidaka, TiO_2-assisted photodegradation of dyes: a study of two competitive primary processes in the degradation of RB in an aqueous TiO_2 colloidal solution, J. Mol. Catal. Chem. 129 (1998) 257–268.
[13] B. Zielinska, J. Grzechulska, B. Grzmil, A.W. Morawski, Photocatalytic degradation of reactive Black 5: a comparison between TiO_2-Tytanpol A11 and TiO_2-degussa P25 photocatalysts, Appl. Catal. B Environ. 35 (2001) L1–L7.
[14] U.G. Akpan, B.H. Hameed, Parameters affecting the photocatalytic degradation of dyes using TiO_2-based photocatalysts: a review, J. Hazard Mater. 170 (2009) 520–529.
[15] M. Arabatzis, T. Stergiopoulos, D. Andreeva, S. Kitova, S.G. Neophytides, P. Falaras, Characterization and photocatalytic activity of Au/TiO_2 thin films for azo-dye degradation, J. Catal. 220 (2003) 127–135.
[16] B. Tian, J. Zhang, T. Tong, F. Chen, Preparation of Au/TiO_2 catalysts from Au(I)-thiosulfate complex and study of their photocatalytic activity for the degradation of methyl orange, Appl. Catal. B Environ. 79 (2008) 394–401.
[17] A. Pandikumar, S. Murugesan, R. Ramaraj, Functionalized silicate sol-gel-supported TiO_2-Au core-shell nanomaterials and their photoelectrocatalytic activity, ACS Appl Mater Interfac. 2 (2010) 1912–1917.
[18] A. Pandikumar, S. Manonmani, R. Ramaraj, TiO_2–Au nanocomposite materials embedded in polymer matrices and their application in the photocatalytic reduction of nitrite to ammonia, Catal Sci Technol 2 (2012) 345–353.
[19] A. Pandikumar, R. Ramaraj, Titanium dioxide–gold nanocomposite materials embedded in silicate sol–gel film catalyst for simultaneous photodegradation of hexavalent chromium and methylene blue, J. Hazard Mater. 203–204 (2012) 244–250.
[20] K.Ö. Hamaloğlu, E. Sağ, A. Tuncel, Bare, gold and silver nanoparticle decorated, monodisperse-porous titania microbeads for photocatalytic dye degradation in a newly constructed microfluidic, photocatalytic packed-bed reactor, J Photoch Photobio A 332 (2017) 60–65.
[21] F. Moreau, G.C. Bond, Preparation and reactivation of Au/TiO_2 catalysts, Catal. Today 122 (2007) 260–265.
[22] L.Q. Jing, S.D. Li, S. Song, L.P. Xue, H.G. Fu, Investigation on the electron transfer between anatase and rutile in nano-sized TiO_2 by means of surface photovoltage technique and its effects on the photocatalytic activity, Sol. Energy Mater. Sol. Cell. 92 (2008) 1030–1036.
[23] P.V. Kamat, Photophysical, photochemical and photo-catalytic aspects of metal nanoparticles, J. Phys. Chem. B 106 (2002) 7729–7744.
[24] L. Sun, J. Li, C. Wang, S. Li, Y. Lai, H. Chen, C. Lin, Ultrasound aided photochemical synthesis of Ag loaded TiO_2 nanotube arrays to enhance photocatalytic activity, J. Hazard Mater. 171 (2009) 1045–1050.
[25] J. Li, Suyoulema, W. Wang, Sarina, A study of photodegradation of sulforhodamine B on Au–TiO_2/bentonite under UV and visible light irradiation, Solid State Sci. 11 (2009) 2037–2043.
[26] C.G. Silva, R. Juarez, T. Marino, R. Molinari, H. Garcıa, Influence of excitation wavelength (UV or visible light) on the photocatalytic activity of titania containing gold nanoparticles for the generation of hydrogen or oxygen from water, J. Am. Chem. Soc. 133 (2011) 595–602.
[27] A. Primo, A. Corma, H. Garcia, Titania supported gold nanoparticles as photocatalyst, Phys. Chem. Chem. Phys. 13 (2011) 886–910.